COMPDYN 2011
ECCOMAS Thematic Conference on
Computational Methods in Structural Dynamics and Earthquake Engineering
M. Papadrakakis, M. Fragiadakis, V. Plevris (eds.)
Corfu, Greece, 25-28 May 2011

SEISMIC WAVE PROPAGATION AND PERFECTLY MATCHED LAYERS USING GFDM

F. Ureña[1], J.J. Benito[2], E. Salete[2] and L. Gavete[3]

[1]Universidad de Castilla-La Mancha
Avda. Camilo José Cela s/n, 13071, Ciudad Real, Spain
francisco.urena@uclm.es

[2]Universidad Nacional de Eduacación a Distancia
Apdo. de correos 60149, 28080 Madrid, Spain
jbenito@ind.uned.es, esalete@ind.uned.es

[3]Universidad Politécnica de Madrid
C/ Alenza 4, 28003 Madrid, Spain
lu.gavete@upm.es

Keywords: meshless methods, generalized finite difference method, moving least squares, seismic waves, perfectly matched layer.

Abstract. *The interior of the Earth is heterogeneous with different material and may have complex geometry. The free surface can also be uneven. Therefore, the use of a meshless method with the possibility of using and irregular grid-point distribution can be interest for modelling this kind of problem.*
This paper shows the application of Generalized Finite Difference Method (GFDM) to the problem of seismic wave propagation in 2-D. To use this method in unbounded domains one must truncate the computational grid-point avoiding reflection from the edges. Perfectly Matched Layers (PML) absorbing boundary condition has then been included in the numerical model proposed in this work.

1 Introduction

During recent years, meshless methods have emerged as a class of effective numerical methods which are capable of avoiding the difficulties encountered in conventional computational mesh based methods. Considerable research in computational mechanics has been devoted to the development of meshless methods. In these methods, the domain of interest is discretized by a scattered set of points.

An important path in the evolution of meshless methods has been the development of the Generalized Finite Difference Method (GFDM), also called Meshless Finite Difference Method (MFDM). The bases of the GFD were published in the early seventies. The idea of using an eight node star and weighting functions to obtain finite difference formulae for irregular meshes, was first put forward by [9] using moving least squares (MLS) interpolation and an advanced version of the GFDM was given by [12]. [1] reported that the solution of the generalized finite difference method depends on the number of nodes in the cloud, the relative coordinates of the nodes with respect to the star node, and on the weight function employed.

An h-adaptive method in GFDM is described in [2], [4] and [5].

In this paper, this meshless method is applied to seismic wave propagation. The GFDM is a robust numerical method applicable to structurally complex media. Due to its relative accuracy and computational efficiency it is the dominant method in modeling earthquake motion [10] and [11]. The perfectly matched layer (PML) absorbing boundary performs more efficiently and more accurately than most traditional or differential equation-based absorbing boundaries ([6], [7], [13] and [8]).

The paper is organized as follows. Section 1 is an introduction. Section 2 describes the GFDM obtaining the explicit generalized differences schemes for the seismic waves propagation. In Section 3 a stability condition is obtained. In Section 4 the grid dispersion relations is derived. In Section 5 are analyzed the relations between irregularity of cloud of nodes, the step of time and star-dispersion. In Section 6 an PML is defined in 2-D. In Section 7 some numerical results are included. Finally, in Section 8 some conclusions are given.

2 Explicit Generalized Differences Schemes for the seismic waves propagation problem for a perfectly elastic, homogeneous and isotropic medium

2.1 Equation of motion

The equations of motion for a perfectly elastic, homogeneous, isotropic medium in 2-D are

$$\left\{\begin{array}{l} \dfrac{\partial^2 U_x(x,y,t)}{\partial t^2} = \alpha^2 \dfrac{\partial^2 U_x(x,y,t)}{\partial x^2} + \beta^2 \dfrac{\partial^2 U_x(x,y,t)}{\partial y^2} + (\alpha^2-\beta^2)\dfrac{\partial^2 U_y(x,y,t)}{\partial x \partial y} \\ \dfrac{\partial^2 U_y(x,y,t)}{\partial t^2} = \beta^2 \dfrac{\partial^2 U_y(x,y,t)}{\partial x^2} + \alpha^2 \dfrac{\partial^2 U_y(x,y,t)}{\partial y^2} + (\alpha^2-\beta^2)\dfrac{\partial^2 U_x(x,y,t)}{\partial x \partial y} \end{array}\right. \tag{1}$$

with the initial conditions

$$U_x(x,y,0) = f_1(x,y); U_y(x,y,0) = f_2(x,y)$$
$$\frac{\partial U_x(x,y,0)}{\partial t} = f_3(x,y); \frac{\partial U_y(x,y,0)}{\partial t} = f_4(x,y) \tag{2}$$

and the boundary condition

$$\left\{\begin{array}{l} a_1 U_x(x_0,y_0,t) + b_1 \frac{\partial U_x(x_0,y_0,t)}{\partial n} = g_1(t) \\ a_2 U_y(x_0,y_0,t) + b_2 \frac{\partial U_y(x_0,y_0,t)}{\partial n} = g_2(t) \end{array}\right. \quad en \quad \Gamma \tag{3}$$

where $f_1(x,y)$, $f_2(x,y)$, $f_3(x,y)$, $f_4(x,y)$, $g_1(t)$ y $g_2(t)$ are showed functions,

$$\alpha = \sqrt{\frac{\lambda + 2\mu}{\rho}}, \quad \beta = \sqrt{\frac{\mu}{\rho}}$$

ρ is the density, λ and μ are Lamé elastic coefficients and Γ is the boundary of Ω.

2.2 A GFDM Explicit Scheme

The aim is to obtain explicit linear expressions for the approximation of partial derivatives in the points of the domain. First of all, an irregular grid or cloud of points is generated in the domain $\Omega \cup \Gamma$. On defining the central node with a set of nodes surrounding that node, the star then refers to a group of established nodes in relation to a central node. Every node in the domain has an associated star assigned to it.
This scheme uses the central-difference form for the time derivative

$$\frac{\partial^2 U_x(x_0,y_0,n\triangle t)}{\partial t^2} = \frac{u_{x,0}^{n+1} - 2u_{x,0}^{n} + u_{x,0}^{n-1}}{(\triangle t)^2}; \qquad \frac{\partial^2 U_y(x_0,y_0,n\triangle t)}{\partial t^2} = \frac{u_{y,0}^{n+1} - 2u_{y,0}^{n} + u_{y,0}^{n-1}}{(\triangle t)^2} \tag{4}$$

Following [1], [2] and [4], the explicit difference formulae for the spatial derivatives are obtained,

$$\begin{aligned}
\frac{\partial^2 U_x(x_0,y_0,n\triangle t)}{\partial x^2} &= -m_0 u_{x,0}^n + \sum_{j=1}^{N} m_j u_{x,j}^n; \quad \frac{\partial^2 U_y(x_0,y_0,n\triangle t)}{\partial x^2} = -m_0 u_{y,0}^n + \sum_{j=1}^{N} m_j u_{y,j}^n \\
\frac{\partial^2 U_x(x_0,y_0,n\triangle t)}{\partial y^2} &= -\eta_0 u_{x,0}^n + \sum_{j=1}^{N} \eta_j u_{x,j}^n; \quad \frac{\partial^2 U_y(x_0,y_0,n\triangle t)}{\partial y^2} = -\eta_0 u_{y,0}^n + \sum_{j=1}^{N} \eta_j u_{y,j}^n \\
\frac{\partial^2 U_x(x_0,y_0,n\triangle t)}{\partial x \partial y} &= -\zeta_0 u_{x,0}^n + \sum_{j=1}^{N} \zeta_j u_{x,j}^n; \quad \frac{\partial^2 U_y(x_0,y_0,n\triangle t)}{\partial x \partial y} = -\zeta_0 u_{y,0}^n + \sum_{j=1}^{N} \zeta_j u_{y,j}^n
\end{aligned} \tag{5}$$

where N is the number of nodes in the star whose central node has the coordinates (x_0, y_0) (in this work $N = 8$ and the are selected by using the four quadrants criteria ([**?**])).
m_0, η_0, ζ_0 are the coefficients that multiply the approximate values of the functions U and V at the central node for the time $n\triangle t$ (u_0^n and v_0^n respectively) in the generalized finite difference explicit expressions for the space derivatives.
m_j, η_j, ζ_j are the coefficients that multiply the approximate values of the functions U and V at the rest of the star nodes for the time $n\triangle t$ (u_j^n and v_j^n respectively) in the generalized finite difference explicit expressions for the space derivatives.
The replacement in Eq. 1 of the explicit expressions obtained for the partial derivatives leads to

$$\begin{cases} u_{x,0}^{n+1} = 2u_{x,0}^{n} - u_{x,0}^{n-1} + (\triangle t)^2[\alpha^2(-m_0 u_{x,0}^n + \sum_1^N m_j u_{x,j}^n) + \beta^2(-\eta_0 u_{x,0}^n + \sum_1^N \eta_j u_{x,j}^n) \\ \qquad +(\alpha^2-\beta^2)(-\zeta_0 u_{y,0}^n + \sum_1^N \zeta_j u_{y,j}^n)] \\ u_{y,0}^{n+1} = 2u_{y,0}^{n} - u_{y,0}^{n-1} + (\triangle t)^2[\beta^2(-m_0 u_{y,0}^n + \sum_1^N m_j u_{y,j}^n) + \alpha^2(-\eta_0 u_{y,0}^n + \sum_1^N \eta_j u_{y,j}^n) \\ \qquad +(\alpha^2-\beta^2)(-\zeta_0 u_{x,0}^n + \sum_1^N \zeta_j u_{x,j}^n)] \end{cases} \tag{6}$$

3 Stability Criterion

For the stability analysis the first idea is to make a harmonic decomposition of the approximated solution at grid points and at a given time level (n). Then we can write the finite difference approximation in the nodes of the star at time n, as

$$u_0^n = A\xi^n e^{i\boldsymbol{k}^T\boldsymbol{x_0}}; \quad u_j^n = A\xi^n e^{i\boldsymbol{k}^T\boldsymbol{x_j}}; \quad v_0^n = B\xi^n e^{i\boldsymbol{k}^T\boldsymbol{x_0}}; \quad v_j^n = B\xi^n e^{i\boldsymbol{k}^T\boldsymbol{x_j}} \tag{7}$$

where $\boldsymbol{x_0}$ is the position vector of the central node of the star, $\boldsymbol{x_j}, j = 1, \cdots, N$ are the position vectors of the rest of the nodes in the star and $\boldsymbol{h_j}$ are the relative position vectors of the nodes in the star in respect to the central node whose coordinates are $h_{jx} = x_j - x_0, h_{jy} = y_j - y_0$. ξ is the amplification factor whose value will determine the stability condition, w is the angular frequency in the grid.

$$\boldsymbol{x_j} = \boldsymbol{x_0} + \boldsymbol{h_j}; \qquad \xi = e^{-iw\triangle t}$$

$\boldsymbol{k}$ (fig. 1) is the column vector of the wave numbers

$$\boldsymbol{k} = \left\{ \begin{array}{c} k_x \\ k_y \end{array} \right\} = k \left\{ \begin{array}{c} \cos\varphi \\ \sin\varphi \end{array} \right\}$$

Then we can write the stability condition as: $\|\xi\| \leq 1$.

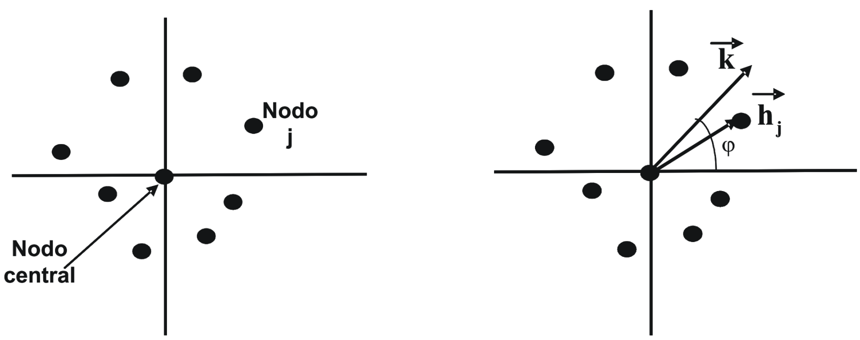

Figure 1: Irregular star (9 nodes) The wavenumber $\vec{\boldsymbol{k}}$

Including 7 into 6, cancelation of $\xi^n e^{i\boldsymbol{\nu}^T \boldsymbol{x_0}}$, leads to

$$A\xi = 2A - \frac{A}{\xi} + (\triangle t)^2[\alpha^2(-Am_0 + A\sum_1^N m_j e^{i\boldsymbol{k}^T \boldsymbol{h_j}}) + \beta^2(-A\eta_0 + A\sum_1^N \eta_j e^{i\boldsymbol{k}^T \boldsymbol{h_j}}) + (\alpha^2 - \beta^2)(-B\zeta_0 + B\sum_1^N \zeta_j e^{i\boldsymbol{k}^T \boldsymbol{h_j}})]$$

$$B\xi = 2B - \frac{B}{\xi} + (\triangle t)^2[\beta^2(-Bm_0 + B\sum_1^N m_j e^{i\boldsymbol{k}^T \boldsymbol{h_j}}) + \alpha^2(-B\eta_0 + B\sum_1^N \eta_j e^{i\boldsymbol{k}^T \boldsymbol{h_j}}) + (\alpha^2 - \beta^2)(-A\zeta_0 + A\sum_1^N \zeta_j e^{i\boldsymbol{k}^T \boldsymbol{h_j}})] \quad (8)$$

where

$$m_0 = \sum_1^N m_j; \quad \eta_0 = \sum_1^N \eta_j; \quad \zeta_0 = \sum_1^N \zeta_j \quad (9)$$

Including 9 into 8, the system of equations is obtained

$$A[\xi - 2 + \frac{1}{\xi} + (\triangle t)^2\alpha^2\sum_1^N m_j(1 - e^{i\boldsymbol{k}^T \boldsymbol{h_j}}) + (\triangle t)^2\beta^2\sum_1^N \eta_j(1 - e^{i\boldsymbol{k}^T \boldsymbol{h_j}})] + B(\triangle t)^2(\alpha^2 - \beta^2)\sum_1^N \zeta_j(1 - e^{i\boldsymbol{k}^T \boldsymbol{h_j}}) = 0$$

$$A(\triangle t)^2(\alpha^2 - \beta^2)\sum_1^N \zeta_j(1 - e^{i\boldsymbol{k}^T \boldsymbol{h_j}}) + B[\xi - 2 + \frac{1}{\xi} + (\triangle t)^2\beta^2\sum_1^N m_j(1 - e^{i\boldsymbol{k}^T \boldsymbol{h_j}}) + (\triangle t)^2\alpha^2\sum_1^N \eta_j(1 - e^{i\boldsymbol{k}^T \boldsymbol{h_j}})] = 0 \quad (10)$$

B can be obtained from the second equation and included into the first, then operating with the real and imaginary parts of conditions obtained, and canceling with conservative criteria, the condition for stability of star is obtained.

$$\triangle t < \sqrt{\frac{4}{(\alpha^2 + \beta^2)[(|m_0| + |\eta_0|) + \sqrt{(m_0 + \eta_0)^2 + \zeta_0^2}]}} \quad (11)$$

4 Star dispersion

4.1 Star-dispersion relations for the P and S waves

The real part of the condition obtained from Eq. 10 leads to

$$\omega = \frac{1}{\triangle t}\arccos\Phi \quad (12)$$

where

$$\Phi = 1 - \frac{(\triangle t)^2}{4}((\alpha^2+\beta^2)(a_1+a_3) + ((\alpha^2+\beta^2)^2(a_1+a_3)^2 +$$
$$4[(\alpha^2-\beta^2)^2(a_5^2-a_6^2) + (\alpha^2 a_2+\beta^2 a_4)(\beta^2 a_2+\alpha^2 a_4) - (\alpha^2 a_1+\beta^2 a_3)(\beta^2 a_1+\alpha^2 a_3)])^{\frac{1}{2}}) \tag{13}$$

with

$$a_1 = \sum_1^N m_j(1-\cos \boldsymbol{k}^T\boldsymbol{h_j}) \Rightarrow \frac{\partial a_1}{\partial k} = a_{1,k} = \sum_1^N m_j d \sin kd$$
$$a_2 = \sum_1^N m_j \sin \boldsymbol{k}^T\boldsymbol{h_j} \Rightarrow \frac{\partial a_2}{\partial k} = a_{2,k} = \sum_1^N m_j d \cos kd$$
$$a_3 = \sum_1^N \eta_j(1-\cos \boldsymbol{k}^T\boldsymbol{h_j}) \Rightarrow \frac{\partial a_3}{\partial k} = a_{3,k} = \sum_1^N \eta_j d \sin kd$$
$$a_4 = \sum_1^N \eta_j \sin \boldsymbol{k}^T\boldsymbol{h_j} \Rightarrow \frac{\partial a_4}{\partial k} = a_{4,k} = \sum_1^N \eta_j d \cos kd$$
$$a_5 = \sum_1^N \zeta_j(1-\cos \boldsymbol{k}^T\boldsymbol{h_j}) \Rightarrow \frac{\partial a_5}{\partial k} = a_{5,k} = \sum_1^N \zeta_j d \sin kd$$
$$a_6 = \sum_1^N \zeta_j \sin \boldsymbol{k}^T\boldsymbol{h_j} \Rightarrow \frac{\partial a_6}{\partial k} = a_{6,k} = \sum_1^N \zeta_j d \cos kd \tag{14}$$

and

$$\boldsymbol{k}^T\boldsymbol{h_j} = k(h_{jx}\cos\varphi + h_{jy}\sin\varphi) = kd$$

Is known that

$$\omega = 2\pi \frac{c^{grid}}{\lambda^{grid}} \tag{15}$$

where c^{grid} and λ^{grid} are the phase velocity (α^{grid} or β^{grid}) and the wavelength (λ_P^{grid} or λ_S^{grid}) in the star respectively.
Defining the relations:

$$s = \frac{2}{\lambda_S^{grid}\sqrt{(r^2+1)[(|m_0|+|\eta_0|)+\sqrt{(m_0+\eta_0)^2+\zeta_0^2}]}} \tag{16}$$

$$s_P = \frac{2}{\lambda_P^{grid}\sqrt{(r^2+1)[(|m_0|+|\eta_0|)+\sqrt{(m_0+\eta_0)^2+\zeta_0^2}]}} \tag{17}$$

$$p = \frac{\beta\triangle t\sqrt{(r^2+1)[(|m_0|+|\eta_0|)+\sqrt{(m_0+\eta_0)^2+\zeta_0^2}]}}{2} \tag{18}$$

$$r = \frac{\alpha}{\beta} \tag{19}$$

$$s_P = \frac{s}{r} \tag{20}$$

Substituting Eqs. 12, 17, 18 and 20 into Eq. 15, the star-dispersion relations for P and S waves are obtained:

$$\frac{\alpha^{grid}}{\alpha} = \frac{\arccos \Phi}{2\pi sp} \tag{21}$$

$$\frac{\beta^{grid}}{\beta} = \frac{\arccos \Phi}{2\pi sp} \tag{22}$$

4.2 Star-dispersion for group velocity

By definition the group velocity is the derivative of w (see Eq.12) with respect to k, thus

$$\alpha^{grid}_{group} = \frac{\partial w}{\partial k} = \frac{\triangle t}{4} \frac{\beta^2 \Upsilon}{\sqrt{1-\Phi^2}} \tag{23}$$

where

$$\begin{aligned}\Upsilon = (r^2+1)(a_{1,k}+a_{3,k}) + \frac{1}{2}[2(r^2+1)^2(a_1+a_3)(a_{1,k}+a_{3,k})+ \\ 4[2(r^2-1)^2(a_5 a_{5,k} - a_6 a_{6,k}) + (r^2 a_{2,k} + a_{4,k})(a_2 + r^2 a_4)+ \\ (r^2 a_2 + a_4)(a_{2,k} + r^2 a_{4,k}) - (r^2 a_{1,k} + a_{3,k})(a_1 + r^2 a_3)- \\ (r^2 a_1 + a_3)(a_{1,k} + r^2 a_{3,k})]] \times [(r^2+1)^2(a_1+a_3)^2+ \\ 4[(r^2-1)^2(a_5^2 - a_6^2) + (r^2 a_2 + a_4)(a_2 + r^2 a_4) - (r^2 a_1 + a_3)(a_1 + r^2 a_3)]]^{-\frac{1}{2}}\end{aligned} \tag{24}$$

Defining

$$\begin{aligned}F = (r^2+1)(a_1+a_3) + [(r^2+1)^2(a_1+a_3)^2+ \\ 4[(r^2-1)^2(a_5^2 - a_6^2) + (r^2 a_2 + a_4)(a_2 + r^2 a_4) - (r^2 a_1 + a_3)(a_1 + r^2 a_3)]]^{\frac{1}{2}}]\end{aligned} \tag{25}$$

and substituting Eqs. 18 and 25 into Eq. 23, the star-dispersion for waves P and S are

$$\frac{\alpha^{grid}_{group}}{\alpha} = \frac{1}{2\sqrt{2}r} \frac{\Upsilon}{\sqrt{F - (\frac{pF}{\sqrt{(r^2+1)[(|m_0| + |\eta_0|) + \sqrt{(m_0+\eta_0)^2 + \zeta_0^2}]}\sqrt{2}})^2}} \tag{26}$$

$$\frac{\beta^{grid}_{group}}{\beta} = \frac{1}{2\sqrt{2}} \frac{\Upsilon}{\sqrt{F - (\frac{pF}{\sqrt{(r^2+1)[(|m_0| + |\eta_0|) + \sqrt{(m_0+\eta_0)^2 + \zeta_0^2}]}\sqrt{2}})^2}} \tag{27}$$

5 Irregularity of the star (IIS) and dispersion

In this section we are going to define the index of irregularity of a star (IIS) and also the index of irregularity of a cloud of nodes (IIC).
The coefficients m_0, η_0, ζ_0 are functions of: a) the number of nodes in the star, b) the coordinates of each star node referred to the central node of the star and c) the weighting function (see references $[1, 4]$). If the number of nodes by star is fixed, in this case 9 ($N = 8$), and the weighting function

$$w(h_{jx}, h_{jy}) = \frac{1}{(\sqrt{h_{jx}^2 + h_{jy}^2})^3} \tag{28}$$

the expression

$$\frac{1}{\sqrt{(r^2+1)[(|m_0| + |\eta_0|) + \sqrt{(m_0+\eta_0)^2 + \zeta_0^2}]}} \tag{29}$$

is function of the coordinates of each node of star referred to its central node.
The coefficients m_0, η_0, ζ_0, are functions of $\frac{1}{h_{jx}^2 + h_{jy}^2}$.
Denoting τ_l a the average of the distances between of the nodes of the star l and its central node and denoting τ the average of the τ_l values in the stars of the mesh, then

$$\boldsymbol{h_j} = \tau \left\{ \begin{array}{c} \overline{h_{jx}} \\ \overline{h_{jy}} \end{array} \right\} \tag{30}$$

$$\overline{m_0} = m_0\tau^2; \quad \overline{\eta_0} = \eta_0\tau^2; \quad \overline{\zeta_0} = \zeta_0\tau^2 \tag{31}$$

The stability criterion can be rewritten

$$\triangle t < \frac{2\tau}{\beta\sqrt{(r^2+1)}\sqrt{(|\overline{m_0}| + |\overline{\eta_0}|) + \sqrt{(\overline{m_0}+\overline{\eta_0})^2 + \overline{\zeta_0}^2}}} \tag{32}$$

For the regular mesh case, the inequality 32 is

$$\triangle t < \frac{\tau}{\beta\sqrt{r^2+1}} \frac{2(\sqrt{2}-1)\sqrt{3}}{\sqrt{5}} \tag{33}$$

Multiplying the right-hand side of inequality 35 by the factor

$$\frac{\sqrt{5}(\sqrt{2}+1)}{\sqrt{3(|\overline{m_0}| + |\overline{\eta_0}| + \sqrt{(\overline{m_0}+\overline{\eta_0})^2 + \overline{\zeta_0}^2})}} \tag{34}$$

the inequality 32 is obtained.
For each one of the stars of the cloud of nodes, we define the IIS for a star with central node in (x_0, y_0) as Eq. 34

$$IIS_{(x_0,y_0)} = \frac{\sqrt{5}(\sqrt{2}+1)}{\sqrt{3(|\overline{m_0}| + |\overline{\eta_0}| + \sqrt{(\overline{m_0}+\overline{\eta_0})^2 + \overline{\zeta_0}^2})}} \tag{35}$$

that takes the value of one in the case of a regular mesh and $0 < IIS \leq 1$
If the index IIS decreases, then absolute values of $\overline{m_0}, \overline{\eta_0}, \overline{\zeta_0}$ increases and then according with 33, $\triangle t$ decreases and star dispersion increases (see 21, 22, 26 and 27).
The irregularity index of a cloud of nodes (IIC) is defined as the minimum of all the IIS of the stars of a cloud of nodes

$$IIC = min\{IIS_{(x_z,y_z)}/z = 1, \cdots, NT\} \tag{36}$$

where NT is the total number of nodes of the domain.

6 Recursive Equations

6.1 Recursive equations with PML in x-direction.

For computational convenience, we split the second order equations of motion (1) into five coupled first order equations by introducing the new field variables $\gamma_{xx}, \gamma_{xy}, \gamma_{yy}$

$$\begin{cases} \rho\dfrac{\partial U_x(x,y,t)}{\partial t} = \dfrac{\partial \gamma_{xx}(x,y,t)}{\partial x} + \dfrac{\partial \gamma_{xy}(x,y,t)}{\partial y} \\ \rho\dfrac{\partial U_y(x,y,t)}{\partial t} = \dfrac{\partial \gamma_{xy}(x,y,t)}{\partial x} + \dfrac{\partial \gamma_{yy}(x,y,t)}{\partial y} \\ \dfrac{\partial \gamma_{xx}(x,y,t)}{\partial t} = (\lambda+2\mu)\dfrac{\partial U_x(x,y,t)}{\partial x} + \lambda\dfrac{\partial U_y(x,y,t)}{\partial y} \\ \dfrac{\partial \gamma_{xy}(x,y,t)}{\partial t} = \mu\dfrac{\partial U_x(x,y,t)}{\partial y} + \mu\dfrac{\partial U_y(x,y,t)}{\partial x} \\ \dfrac{\partial \gamma_{yy}(x,y,t)}{\partial t} = \lambda\dfrac{\partial U_x(x,y,t)}{\partial x} + (\lambda+2\mu)\dfrac{\partial U_y(x,y,t)}{\partial y} \end{cases} \tag{37}$$

We shall make two simplifications, we shall assume that the space far from the region of interest is homogeneous, linear and time invariant.Then, under these assumptions, the radiating solution in infinite space must be (superposition of plane waves):

$$\boldsymbol{\omega}(\boldsymbol{x},t) = \boldsymbol{W}(\boldsymbol{x},t)e^{i(\boldsymbol{\kappa}\cdot\boldsymbol{x}-wt)} \tag{38}$$

As w is an analytic function of $\boldsymbol{x}$,then we can analytically continue it, evaluating the solution at complex values of $\boldsymbol{x}$. Then, the solution is not changed in the region of interest and the reflections are avoided.

$$\begin{cases} U_x(x,y,t) = u_x(x,y)e^{-iwt} \Rightarrow \dot{U}_x(x,y,t) = -iwu_x(x,y)e^{-iwt} = -iwU_x(x,y,t) \\ U_y(x,y,t) = u_y(x,y)e^{-iwt} \Rightarrow \dot{U}_y(x,y,t) = -iwu_y(x,y)e^{-iwt} = -iwU_y(x,y,t) \\ \gamma_{xx}(x,y,t) = \Gamma_{xx}(x,y)e^{-iwt} \Rightarrow \dot{\gamma}_{xx}(x,y,t) = -iw\Gamma_{xx}(x,y)e^{-iwt} = -iw\gamma_{xx}(x,y,t) \\ \gamma_{xy}(x,y,t) = \Gamma_{xy}(x,y)e^{-iwt} \Rightarrow \dot{\gamma}_{xy}(x,y,t) = -iw\Gamma_{xy}(x,y)e^{-iwt} = -iw\gamma_{xy}(x,y,t) \\ \gamma_{yy}(x,y,t) = \Gamma_{yy}(x,y)e^{-iwt} \Rightarrow \dot{\gamma}_{yy}(x,y,t) = -iw\Gamma_{yy}(x,y)e^{-iwt} = -iw\gamma_{yy}(x,y,t) \end{cases} \tag{39}$$

Thus, we have a complex coordinate

$$\tilde{x} = x + if \tag{40}$$

As this complex coordinate is inconvenient, we have a change variables in this region (PML)

$$\partial\tilde{x} = (1 + i\frac{df}{dx})\partial x \tag{41}$$

In order to have an attenuation rate in the PML independent of frequency (ω), we have

$$\frac{df}{dx} = \frac{\delta_x(x)}{\omega} \tag{42}$$

where ω is the angular frequency and δ_x is some function of x.
PML x-dir can be conceptually assumed up by a single transformation of the original equation. Then wherever an x derivative appears in the wave equations, it is replaced in the form

$$\frac{\partial}{\partial x} \to \frac{1}{1 + i\frac{\delta_x(x)}{w}}\frac{\partial}{\partial x} \tag{43}$$

The equations are fecuency-dependent, and to advoid it a solution is to use an auxiliary differential equation (ADE) approach in the implementation of PML. The following equations are obtained

$$\begin{cases}
\frac{\partial U_x(x,y,t)}{\partial t} = \frac{1}{\rho}[\frac{\partial \gamma_{xx}(x,y,t)}{\partial x} + \frac{\partial \gamma_{xy}(x,y,t)}{\partial y}] + \psi_1(x,y,t) - \delta_x U_x(x,y,t) \\
\frac{\partial U_y(x,y,t)}{\partial t} = \frac{1}{\rho}[\frac{\partial \gamma_{xy}(x,y,t)}{\partial x} + \frac{\partial \gamma_{yy}(x,y,t)}{\partial y}] + \psi_2(x,y,t) - \delta_x U_y(x,y,t) \\
\frac{\partial \gamma_{xx}(x,y,t)}{\partial t} = (\lambda + 2\mu)\frac{\partial U_x(x,y,t)}{\partial x} + \lambda\frac{\partial U_y(x,y,t)}{\partial y} + \psi_3(x,y,t) - \delta_x \gamma_{xx}(x,y,t) \\
\frac{\partial \gamma_{xy}(x,y,t)}{\partial t} = \mu\frac{\partial U_x(x,y,t)}{\partial y} + \mu\frac{\partial U_y(x,y,t)}{\partial x} + \psi_4(x,y,t) - \delta_x \gamma_{xy}(x,y,t) \\
\frac{\partial \gamma_{yy}(x,y,t)}{\partial t} = \lambda\frac{\partial U_x(x,y,t)}{\partial x} + (\lambda + 2\mu)\frac{\partial U_y(x,y,t)}{\partial y} + \psi_5(x,y,t) - \delta_x \gamma_{yy}(x,y,t) \\
\frac{\partial \psi_1(x,y,t)}{\partial t} = \frac{\delta_x}{\rho}\frac{\partial \gamma_{xy}(x,y,t)}{\partial y} \\
\frac{\partial \psi_2(x,y,t)}{\partial t} = \frac{\delta_x}{\rho}\frac{\partial \gamma_{yy}(x,y,t)}{\partial y} \\
\frac{\partial \psi_3(x,y,t)}{\partial t} = \lambda\delta_x\frac{\partial U_y(x,y,t)}{\partial y} \\
\frac{\partial \psi_4(x,y,t)}{\partial t} = \mu\delta_x\frac{\partial U_x(x,y,t)}{\partial y} \\
\frac{\partial \psi_5(x,y,t)}{\partial t} = (\lambda + 2\mu)\delta_x\frac{\partial U_y(x,y,t)}{\partial y}
\end{cases} \tag{44}$$

Where the five last equations 46 are ADE approach and the new field variables

$$\begin{cases}
\psi_1(x,y,t) = \frac{1}{\rho}i\frac{\delta_x}{\omega}\frac{\partial \gamma_{xy}(x,y,t)}{\partial y} \\
\psi_2(x,y,t) = \frac{1}{\rho}i\frac{\delta_x}{\omega}\frac{\partial \gamma_{yy}(x,y,t)}{\partial y} \\
\psi_3(x,y,t) = i\lambda\frac{\delta_x}{\omega}\frac{\partial U_y(x,y,t)}{\partial y} \\
\psi_4(x,y,t) = i\mu\frac{\delta_x}{\omega}\frac{\partial U_x(x,y,t)}{\partial y} \\
\psi_5(x,y,t) = i(\lambda + 2\mu)\frac{\delta_x}{\omega}\frac{\partial U_y(x,y,t)}{\partial y}
\end{cases} \tag{45}$$

6.1.1 An scheme in GDFM for elastic part

Following [1], [2] and [4], the explicit difference formulae for the spatial derivatives of a function are obtained,

$$\frac{\partial U_x(x_0,y_0,n\triangle t)}{\partial x} = -m_{1,0}u^n_{x,0}+\sum_{j=1}^{N} m_{1,j}u^n_{x,j}; \quad \frac{\partial U_x(x_0,y_0,n\triangle t)}{\partial y} = -m_{2,0}u^n_{x,0}+\sum_{j=1}^{N} m_{2,j}u^n_{x,j} \tag{46}$$

and similarly for first spatial derivatives of the functions: $U_y, \gamma_{xx}, \gamma_{xy}, \gamma_{yy}, \psi_1, \psi_2, \psi_3, \psi_4, \psi_5$ Substituting Eq. 46 into Eq. 37 the an scheme in GFDM for elastic part are obtained

$$\begin{cases} u^{n+1}_{x,0} = u^n_{x,0} + \dfrac{\triangle t}{\rho}[-m_{1,0}\gamma^n_{xx,0} + \sum_{j=1}^{N} m_{1,j}\gamma^n_{xx,j} - m_{2,0}\gamma^n_{xy,0} + \sum_{j=1}^{N} m_{2,j}\gamma^n_{xy,j}] \\ u^{n+1}_{y,0} = u^n_{y,0} + \dfrac{\triangle t}{\rho}[-m_{1,0}\gamma^n_{xy,0} + \sum_{j=1}^{N} m_{1,j}\gamma^n_{xy,j} - m_{2,0}\gamma^n_{yy,0} + \sum_{j=1}^{N} m_{2,j}\gamma^n_{yy,j}] \\ \gamma^{n+1}_{xx,0} = \gamma^n_{xx,0} + \triangle t[(\lambda+2\mu)(-m_{1,0}u^n_{x,0} + \sum_{j=1}^{N} m_{1,j}u^n_{x,j}) \\ +\lambda(-m_{2,0}u^n_{y,0} + \sum_{j=1}^{N} m_{y,j}u^n_{2,j})] \\ \gamma^{n+1}_{xy,0} = \gamma^n_{xy,0} + \triangle t[\mu(-m_{2,0}u^n_{x,0} + \sum_{j=1}^{N} m_{2,j}u^n_{x,j}) \\ +\mu(-m_{1,0}u^n_{y,0} + \sum_{j=1}^{N} m_{1,j}u^n_{y,j})] \\ \gamma^{n+1}_{yy,0} = \gamma^n_{yy,0} + \triangle t[\lambda(-m_{1,0}u^n_{x,0} + \sum_{j=1}^{N} m_{1,j}u^n_{x,j}) \\ +(\lambda+2\mu)(-m_{2,0}u^n_{y,0} + \sum_{j=1}^{N} m_{2,j}u^n_{y,j})] \end{cases} \tag{47}$$

6.1.2 An scheme in GDFM for PML part

Substituting Eq. 46 into Eq. 44 the an scheme in GFDM for PML part are obtained

$$
\left\{
\begin{array}{l}
u_{x,0}^{n+1} = u_{x,0}^{n} + \dfrac{\triangle t}{\rho}[-m_{1,0}\gamma_{xx,0}^{n} + \displaystyle\sum_{j=1}^{N} m_{1,j}\gamma_{xx,j}^{n} - \\
m_{2,0}\gamma_{xy,0}^{n} + \displaystyle\sum_{j=1}^{N} m_{2,j}\gamma_{xy,j}^{n}] + \triangle t[\psi_{1,0}^{n} - \delta_x u_{x,0}^{n}] \\
u_{y,0}^{n+1} = u_{y,0}^{n} + \dfrac{\triangle t}{\rho}[-m_{1,0}\gamma_{xy,0}^{n} + \displaystyle\sum_{j=1}^{N} m_{1,j}\gamma_{xy,j}^{n} - \\
m_{2,0}\gamma_{yy,0}^{n} + \displaystyle\sum_{j=1}^{N} m_{2,j}\gamma_{yy,j}^{n}] + \triangle t[\psi_{2,0}^{n} - \delta_x u_{y,0}^{n}] \\
\gamma_{xx,0}^{n+1} = \gamma_{xx,0}^{n} + \triangle t[(\lambda+2\mu)(-m_{1,0}u_{x,0}^{n} + \displaystyle\sum_{j=1}^{N} m_{1,j}u_{x,j}^{n}) + \\
\lambda(-m_{2,0}u_{y,0}^{n} + \displaystyle\sum_{j=1}^{N} m_{2,j}u_{y,j}^{n})] + \triangle t[\psi_{3,0}^{n} - \delta_x \gamma_{xx,0}^{n}] \\
\gamma_{xy,0}^{n+1} = \gamma_{xy,0}^{n} + \triangle t[\mu(-m_{2,0}u_{x,0}^{n} + \displaystyle\sum_{j=1}^{N} m_{2,j}u_{x,j}^{n}) + \\
\mu(-m_{1,0}u_{y,0}^{n} + \displaystyle\sum_{j=1}^{N} m_{1,j}u_{y,j}^{n})] + \triangle t[\psi_{4,0}^{n} - \delta_x \gamma_{xy,0}^{n}] \\
\gamma_{yy,0}^{n+1} = \gamma_{yy,0}^{n} + \triangle t[\lambda(-m_{1,0}u_{x,0}^{n} + \displaystyle\sum_{j=1}^{N} m_{1,j}u_{x,j}^{n}) + \\
(\lambda+2\mu)(-m_{2,0}u_{y,0}^{n} + \displaystyle\sum_{j=1}^{N} m_{2,j}u_{y,j}^{n})] + \triangle t[\psi_{5,0}^{n} - \delta_x \gamma_{yy,0}^{n}] \\
\psi_{1,0}^{n+1} = \psi_{1,0}^{n} + \dfrac{\triangle t}{\rho}\delta_x[-m_{2,0}\gamma_{xy,0}^{n} + \displaystyle\sum_{j=1}^{N} m_{2,j}\gamma_{xy,j}^{n}] \\
\psi_{2,0}^{n+1} = \psi_{2,0}^{n} + \dfrac{\triangle t}{\rho}\delta_x[-m_{2,0}\gamma_{yy,0}^{n} + \displaystyle\sum_{j=1}^{N} m_{2,j}\gamma_{yy,j}^{n}] \\
\psi_{3,0}^{n+1} = \psi_{3,0}^{n} + \lambda\triangle t\delta_x[-m_{2,0}u_{y,0}^{n} + \displaystyle\sum_{j=1}^{N} m_{2,j}u_{y,j}^{n}] \\
\psi_{4,0}^{n+1} = \psi_{4,0}^{n} + \mu\triangle t\delta_x[-m_{2,0}u_{x,0}^{n} + \displaystyle\sum_{j=1}^{N} m_{2,j}u_{x,j}^{n}] \\
\psi_{5,0}^{n+1} = \psi_{5,0}^{n} + (\lambda+2\mu)\triangle t\delta_x[-m_{2,0}u_{y,0}^{n} + \displaystyle\sum_{j=1}^{N} m_{2,j}u_{y,j}^{n}]
\end{array}
\right. \tag{48}
$$

6.2 Recursive equations with PML in x-direction and y-direction.

In this case

$$\left\{ \begin{array}{l} \frac{\partial}{\partial x} \to \frac{\partial}{\partial x}(1+i\frac{\delta}{\omega})^{-1} \\ \frac{\partial}{\partial y} \to \frac{\partial}{\partial y}(1+i\frac{\delta}{\omega})^{-1} \end{array} \right. \tag{49}$$

We obtain

$$\left\{ \begin{array}{l} \frac{\partial U_x(x,y,t)}{\partial t} = \frac{1}{\rho}[\frac{\partial \gamma_{xx}(x,y,t)}{\partial x} + \frac{\partial \gamma_{xy}(x,y,t)}{\partial y}] - \delta U_x(x,y,t) \\ \frac{\partial U_y(x,y,t)}{\partial t} = \frac{1}{\rho}[\frac{\partial \gamma_{xy}(x,y,t)}{\partial x} + \frac{\partial \gamma_{yy}(x,y,t)}{\partial y}]) - \delta U_y(x,y,t) \\ \frac{\partial \gamma_{xx}(x,y,t)}{\partial t} = (\lambda+2\mu)\frac{\partial U_x(x,y,t)}{\partial x} + \lambda\frac{\partial U_y(x,y,t)}{\partial y} - \delta\gamma_{xx}(x,y,t) \\ \frac{\partial \tau_{xy}(x,y,t)}{\partial t} = \mu\frac{\partial U_x(x,y,t)}{\partial y} + \mu\frac{\partial U_y(x,y,t)}{\partial x} - \delta\gamma_{xy}(x,y,t) \\ \frac{\partial \gamma_{yy}(x,y,t)}{\partial t} = \lambda\frac{\partial U_x(x,y,t)}{\partial x} + (\lambda+2\mu)\frac{\partial U_y(x,y,t)}{\partial y} - \delta\gamma_{yy}(x,y,t) \end{array} \right. \tag{50}$$

6.2.1 An scheme in GDFM for elastic part

The equations of the elastic part is given by Eq. 47

6.2.2 An scheme in GDFM for PML part

Substituting Eq. 46 into Eq. 50 the an scheme in GFDM for PML part are obtained

$$\left\{ \begin{array}{l} u^{n+1}_{x,0} = u^n_{x,0} + \frac{\triangle t}{\rho}[-m_{1,0}\gamma^n_{xx,0} + \sum_{j=1}^{N} m_{1,j}\gamma^n_{xx,j} - \\ m_{2,0}\gamma^n_{xy,0} + \sum_{j=1}^{N} m_{2,j}\gamma^n_{xy,j}] - \triangle t\delta u^n_{x,0} \\ u^{n+1}_{y,0} = u^n_{y,0} + \frac{\triangle t}{\rho}[-m_{1,0}\gamma^n_{xy,0} + \sum_{j=1}^{N} m_{1,j}\gamma^n_{xy,j} - \\ m_{2,0}\gamma^n_{yy,0} + \sum_{j=1}^{N} m_{2,j}\gamma^n_{yy,j}] - \triangle t\delta u^n_{y,0} \\ \gamma^{n+1}_{xx,0} = \gamma^n_{xx,0} + \triangle t[(\lambda+2\mu)(-m_{1,0}u^n_{x,0} + \sum_{j=1}^{N} m_{1,j}u^n_{x,j}) + \\ \lambda(-m_{2,0}u^n_{y,0} + \sum_{j=1}^{N} m_{y,j}u^n_{y,j})] - \triangle t\delta\gamma^n_{xx,0} \\ \gamma^{n+1}_{xy,0} = \gamma^n_{xy,0} + \triangle t[\mu(-m_{2,0}u^n_{x,0} + \sum_{j=1}^{N} m_{2,j}u^n_{x,j}) + \\ \mu(-m_{1,0}u^n_{y,0} + \sum_{j=1}^{N} m_{1,j}u^n_{y,j})] - \triangle t\delta\gamma^n_{xy,0} \\ \gamma^{n+1}_{yy,0} = \gamma^n_{yy,0} + \triangle t[\lambda(-m_{1,0}u^n_{x,0} + \sum_{j=1}^{N} m_{1,j}u^n_{x,j}) + \\ (\lambda+2\mu)(-m_{2,0}u^n_{y,0} + \sum_{j=1}^{N} m_{2,j}u^n_{y,j})] - \triangle t\delta\gamma^n_{yy,0} \end{array} \right. \tag{51}$$

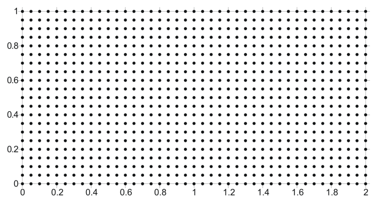

Figure 3 Regular mesh (861 nodes)

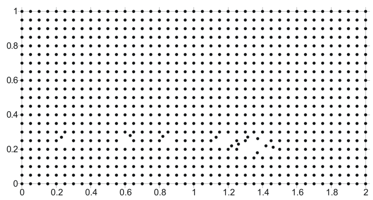

Figure 4 Irregular mesh($IIC = 0.9072$)

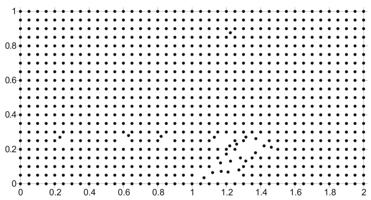

Figure 5 Irregular mesh($IIC = 0.8312$)

7 Numerical Results

7.1 GFDM with known boundary conditions

Let us solve the Eq. 1, in $\Omega = [0,2] \times [0,1] \subset \mathbf{R}^2$, with Dirichlet boundary conditions

$$\begin{cases} U_x(0,y,t) = 0 & \forall y \in [0,1] \\ U_x(1,y,t) = \sin 2 \sin y \cos(\sqrt{2}\beta t) & \forall y \in [0,1] \\ U_x(x,0,t) = 0 & \forall x \in [0,1] \\ U_x(x,1,t) = \sin x \sin 2 \cos(\sqrt{2}\beta t) & \forall x \in [0,1] \end{cases}$$

$$\begin{cases} U_y(0,y,t) = 0 & \forall y \in [0,1] \\ U_y(1,y,t) = \cos 2 \cos y \cos(\sqrt{2}\beta t) & \forall y \in [0,1] \\ U_y(x,0,t) = 0 & \forall x \in [0,1] \\ U_y(x,1,t) = \cos x \cos 2 \cos(\sqrt{2}\beta t) & \forall x \in [0,1] \end{cases} \tag{52}$$

and initial conditions

$$U_x(x,y,0) = \sin x \sin y; U_y(x,y,0) = \cos x \cos y; \quad \frac{\partial U_x(x,y,0)}{\partial t} = 0; \frac{\partial U_y(x,y,0)}{\partial t} = 0 \tag{53}$$

using a regular mesh (see Fig. 3 with 861 nodes) and irregular meshes (see Figs. 4 and 5) with 861 nodes. The analytical solutions (see Fig. 6) is

$$U_x(x,y,t) = \cos(\sqrt{2}\beta t) \sin x \sin y; \quad U_y(x,y,t) = \cos(\sqrt{2}\beta t) \cos x \cos y \tag{54}$$

The weighting function is given by Eq. 29 and the criterion for the selection of star nodes is the quadrant criterion (see references $[1,4,5]$). The global error is evaluated for each time increment, in the last time step considered, using the following formula

$$Global \quad error = \frac{\sqrt{\frac{\sum_{j=1}^{NT} (sol(j) - exac(j))^2}{NT}}}{|exac_{max}|} \times 100 \tag{55}$$

where $sol(j)$ is the GFDM solution at the node j $exac(j)$ is the exact value of the solution at the node j, $exac_{max}$ is the maximum value of the exact solution in the cloud of nodes considered and NT is the total number of nodes of the domain.

Table 1 shows the global error, with $\triangle t = 0.0005$, for value of $\alpha = 1$ and $\beta = 0.5$, in the regular mesh (see Fig. 3) with $n = 500$.

Table 2 shows the values of the global error for several values of $\triangle t$, using the irregular mesh with 861 nodes (see Fig. 4), with $n = 500$ and $IIC = 0.9072$.

Table 3 shows the values of the global error for several values of $\triangle t$, using the irregular mesh with 861 nodes (see Fig. 5), with $n = 500$ and $IIC = 0.8312$.

Table 1: The global errors with $\alpha = 1; \beta = 0.5$

N of Nodes	Global Error U_x	Global Error U_y
861	0.0004222	0.0004712

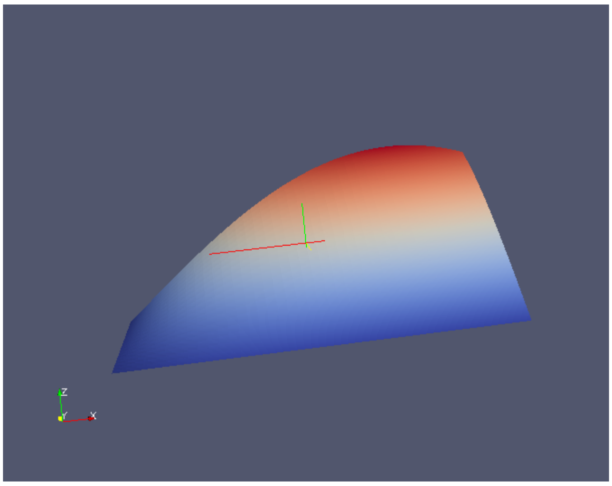

Figure 6: Exact solution U_x without PML.

Table 2: Influence of the $\triangle t$ in the global error with $\alpha = 1; \beta = 0.5; n = 500; IIC = 0.9072$

$\triangle t$	Global Error U_x	Global Error U_y
0.005	0.004105	0.004326
0.001	0.0017170	0.001374
0.0005	0.000662	0.000669

Table 3: Influence of the $\triangle t$ in the global error with $\alpha = 1; \beta = 0.5; n = 500; IIC = 0.8312$

$\triangle t$	Global Error U_x	Global Error U_y
0.005	0.005234	0.005321
0.001	0.001983	0.002110
0.0005	0.000821	0.000840

7.2 GFDM with PML

Let us solve the Eq. 1, in $\Omega = [0,2] \times [0,1] \subset \mathbf{R}^2$, with homogeneous the Dirichlet boundary conditions and the initial conditions are given by Eq. 53, using the regular mesh with 861 nodes (see Fig. 6) used in subsection 7.1, the analytical solutions is given by Eq. 54. The weighting function is given by Eq. 28 and the criterion for the selection of star nodes is the quadrant criterion.

Figure 8 shows the graphic the approximated solution of u_x, after 100 time steps, with PML in x-direction and y-direction for $1.4 \leq x \leq 2$ and $0.6 \leq y \leq 1$ (see Fig. 7).

Figure 10 shows the graphic the approximated solution of u_x, after 100 time steps, with PML

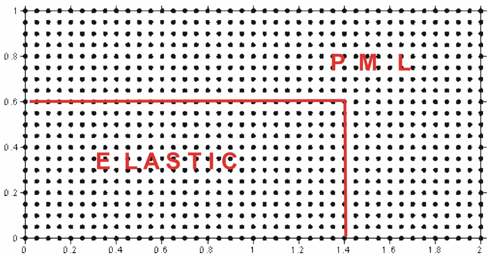

Figure 7: Regular mesh with PML region.

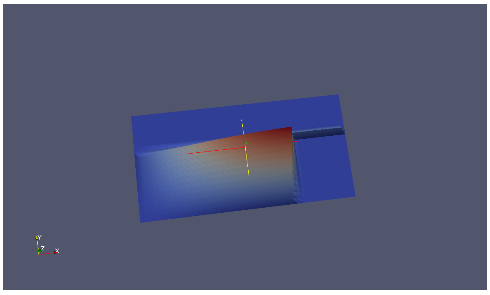

Figure 8: Approximated solution U_x with PML.

in x-direction and y-direction for $\leq x \leq 0.6$ and $0 \leq y \leq 0.2$, $0.8 \leq y \leq 1$ (see Fig. 9).

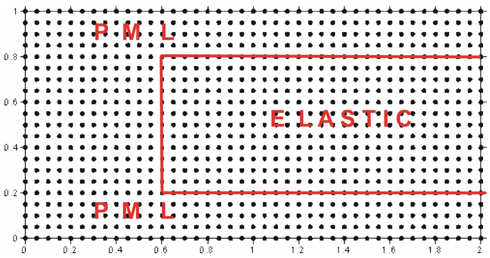

Figure 9: Regular mesh with PML region.

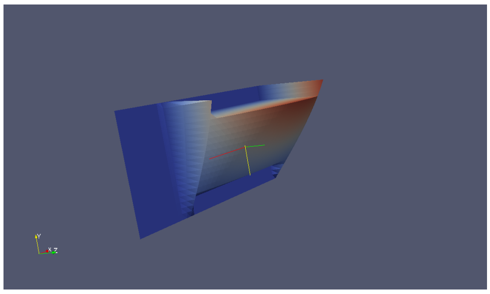

Figure 10: Approximated solution U_x with PML.

8 Conclusions

This paper shows a scheme in generalized finite differences, for seismic wave propagation in 2-D. The von Neumann stability criterion has been expressed as a function of the coefficients of the star equation and the velocity ratio.

The investigated star dispersion has been related with the irregularity of the star using the irregularity indicator of the mesh. The use of irregular meshes, adjusted to the geometry of the problem, may create high dispersion in certain stars which is related to high values of the irregularity index of the mesh (IIC). In this case the mesh can be redefined by an adaptive process ([2]) until a mesh whit suitable dispersion and irregularity index values is obtained.

The formulation of the PML is compatible with GFDM and numerical results confirm that PML has an extraordinary performance in absorbing outgoing waves.

ACKNOWLEGMENTS.

The authors acknowledge the support from Ministerio de Ciencia e Innovación of Spain, project CGL$2008-01757$/CLI.

REFERENCES

[1] J.J. Benito, F. Ureña, L. Gavete, *Influence several factors in the generalized finite difference method*. Applied Mathematical Modeling 25, 1039–1053 (2001).

[2] J.J. Benito, F. Ureña, L. Gavete, R. Alvarez, *An h-adaptive method in the generalized finite difference*. Comput. Methods Appl. Mech. Eng. 192, 735–759 (2003).

[3] J.J. Benito, F. Ureña, L. Gavete, B. Alonso, *Solving parabolic and hyperbolic equations by Generalized Finite Difference Method*. Journal of Computational and Applied Mathematics 209 Issue 2, 208–233 (2007).

[4] J.J. Benito, F. Ureña, L. Gavete, *Leading-Edge Applied Mathematical Modelling Research (chapter 7)*. Nova Science Publishers, New York, (2008).

[5] J.J. Benito, F. Ureña, L. Gavete, B. Alonso, *Application of the Generalized Finite Difference Method to improve the approximated solution of pdes*. Computer Modelling in Engineering & Sciences. 38, 39–58 (2009).

[6] J.P. Berenger, *A perfectly matched layer for the absortion of electromagnetic.* J. Comput. Physics, 114, 185–200, (1994).

[7] W.C. Chew, Q.H. Liu, *Perfectly matched layer for elastodinamycs, a new absorbing boundary condition.* J. Comput. Acoustics, 4, 341–359, (1996).

[8] S.G. Johnson, *Notes on Perfectly Matched Layers (PMLs)*. Courses 18.369 and 18.336 at MIT. July (2008).

[9] T. Liszka, J. Orkisz, *The finite difference method at arbitrary irregular grids and its application in applied mechanics*. Computer & Structures, 83–95, (1980).

[10] P. Moczo, J. Kristek , L. Halada, *The Finite-Difference method for seismologists. An introduction.*. Comenius University Bratislava, 158 pgs.(1994).

[11] P. Moczo, J. Kristek , M. Galis, P. Pazak , M. Balazovjech, *The Finite-Difference and Finite-Element modelling of seismic wave propagation and earthquake motion*. Acta Physica Slovaca, vol. 57 No. 2, 177-406 (2007).

[12] J. Orkisz, *Finite Difference Method. (Part.III) in Handbook of Computational Solid Mechanics*. M. Kleiber (eds.), Springer-Verlag, Berlin, (1998)

[13] E.A. Skelton, S.D.M. Adams, R.V Craster, *Guided elastic waves and perfectly matched layers*. Wave Motion, Elsevier, 44, 573-592 (2007).